Inorganic Chemistry, Vol. 14, No. 8, 1975 **1807**

Contribution from the Technical University of Denmark,
Chemistry Department A, DK-2800 Lyngby, Denmark

Chloro Complexes in Molten Salts. IV. A Potentiometric and Spectrophotometric Study of the System KCl–$FeCl_3$ in the Temperature Range 275–350°

H. A. ANDREASEN and N. J. BJERRUM*

Received November 13, 1974

AIC407788

It was found that the variation in pCl^- from 0.29 to 4.01 in molten $KFeCl_4$ as a function of melt composition (i.e., KCl to $FeCl_3$) could best be explained by the following reactions: $2FeCl_4^- \rightleftarrows Fe_2Cl_7^- + Cl^-$ (1); $Fe_2Cl_7^- \rightleftarrows Fe_2Cl_6 + Cl^-$ (2). The pK values (based on molar concentrations) for reaction 1 were found to be 6.603 ± 0.005, 6.322 ± 0.005, 6.057 ± 0.003, and 5.821 ± 0.005 at 275, 300, 325, and 350°, respectively. Similarily the pK values for reaction 2 were found to be 5.70 ± 0.04, 5.38 ± 0.03, 5.18 ± 0.02, and 5.02 ± 0.04 at 275, 300, 325, and 350°, respectively. From the temperature dependence of equilibrium 1 it was found that in the temperature range 275–350° the value of $\Delta H°$ was 16.33 ± 0.07 kcal/mol and that of $\Delta S°$ was 0.4 ± 0.1 cal/(deg mol). Similarily for equilibrium 2 $\Delta H°$ was found to be 14 ± 1 kcal/mol and $\Delta S°$ was found to be 0 ± 2 cal/(deg mol). The composition of the eutectic mixture of KCl–$FeCl_3$ at 242° was found by an extrapolation procedure to be 51.32 ± 0.02 mol % KCl. All errors given are standard errors. The spectra of $FeCl_4^-$, $Fe_2Cl_7^-$, and Fe_2Cl_6 at 300° were calculated from measured spectra using the above found equilibrium constants. The calculated spectrum of Fe_2Cl_6 was furthermore compared with the measured spectrum of Fe_2Cl_6 in the gas phase at 300°.

Introduction

Despite the rather considerable amount of potentiometric investigations carried out recently on the chloro complexes in the MCl–$AlCl_3$ systems (M = Li, Na, K, Cs),[1-7] no potentiometric work as far as we know has been performed on the MCl–$FeCl_3$ systems. Cook and Dunn[8] have shown that in contrast to the results of two earlier studies[9,10] on the NaCl–$FeCl_3$ system a congruently melting 1:1 compound is present in the NaCl–$FeCl_3$ (and KCl–$FeCl_3$ systems). The same is true for the LiCl–$FeCl_3$ system.[11] The existence of a 1:1 compound is furthermore consistent with the sharp drop in vapor pressure by addition of NaCl to molten $FeCl_3$ up to about 50 mol %. The authors assume that the 1:1 compound contains the $FeCl_4^-$ complex ion. The calorimetric measurements by the same authors also point in the direction of the formation of a $FeCl_4^-$ ion in the melt. Solid compounds containing the $FeCl_4^-$ ion have also been examined.[12,13]

A gas chromatographic investigation of the volatile solute $SbCl_3$ in molten KCl–$FeCl_3$ has been used for proposing the equilibrium $2FeCl_4^- \rightleftharpoons Fe_2Cl_7^- + Cl^-$ in this melt.[14]

In the present work it is shown that, besides the equilibrium $2FeCl_4^- \rightleftarrows Fe_2Cl_7^- + Cl^-$, the equilibrium $FeCl_7^- \rightleftarrows Fe_2Cl_6 + Cl^-$ must also be considered in order to get agreement between measurements and calculations. This is in agreement with the conditions in the NaCl–$AlCl_3$ melts where it was found that the reactions $2AlCl_3 \rightleftarrows Al_2Cl_6$, $AlCl_4^- + AlCl_3 \rightleftarrows Al_2Cl_7^-$, and $2AlCl_4^- \rightleftarrows Al_2Cl_7^- + Cl^-$ fully described the systems.[5]

Experimental Section

Materials and Measurements. $FeCl_3$ was made from pure metal ("Specpure", total metal impurities about 14 ppm) and chlorine (Fluka >99.9%) and further purified by distillation in chlorine gas. KCl (analytical reagent from Riedel-de Haën) was purified by first passing HCl over the solid and then through the melt, flushing with pure N_2, and finally filtering the melt.

The experimental techniques used in the present work are almost the same as those described previously.[6,15] The cells with electrodes were made of Pyrex with vitreous carbon from Carbone-Lorraine fused into the bottom. Chlorine (Fluka >99.9%) was added under a known pressure (0.50 atm) to the cells, which were sealed vacuum-tight. In the temperature range 275–350° the pressure was then about 1 atm. A porous pin from Radiometer (primarily of α-Al_2O_3) separated the two cell compartments. In some cases, in which the mole fraction of KCl was lower than 0.500, the connecting tube between the two cell compartments was sealed after chlorine had been added. In these cases the activity of chlorine probably remained about the same in each compartment, since the solubility of chlorine in chloride melts is rather low (and seems to increase with higher chloride activity and higher temperature of the melt[16]). This should still be so even if there is a somewhat different pressure in the two compartments due to the vapor pressure of the melt. The internal resistances of the operating cells varied in the range 600–1100 Ω depending on the construction of the cells, the temperature, and composition of the melt. The porous pins in the cells had diameters of ca. 1 mm and lengths of ca. 8 mm.

The furnace used for the potentiometric and density measurements was rather similar to the furnace previously described.[6] However, a copper–aluminum alloy (with 90% copper) was used instead of aluminum as the core material. The whole furnace was furthermore mounted on two hollow shafts supported by four ball bearings. The hollow shafts carried cooling water and electric leads to the furnace. In this way the highest degree of mobility was obtained. An electric motor geared down to 14 rpm was used to rock the furnace. The thermocouple signal from the middle part of the furnace, which was heated by the main heating element, was corrected for cold-junction temperature and amplified with a low-level dc amplifier. The error signal was fed to a Eurotherm PID regulator with fast cycling SCR output (LP96). The temperature set point could be changed linearly in time with a stepmotor-driven potentiometer. This arrangement was used in connection with necessary density measurements. The top and bottom heating elements were controlled by a similar regulator operated by the small temperature difference measured by thermocouples placed on the middle and end parts of the furnace. The temperature of the furnace could be controlled within ±0.1° in the range 150–700°. The temperature variation over the middle 200 mm was less than 0.3°.

The potentiometric measurements were performed with an Analogic Type AN 2544 digital panel-meter with resolution 0.1 mV and full scale of 3999.9 mV, when necessary in connection with an Analog Devices Type 260J amplifier, coupled as a 10.000× amplifier. The same system, supplemented with an automatic cold-junction compensation, was used in connection with a calibrated chromel–alumel thermocouple for the temperature measurements.

The density measurements of the used melts were made by an automated "float" method, in which the falling and rising quartz floats—which contained a magnetic material—were detected by a differential transformer.[17]

The material that made up a melt was weighed in a nitrogen-filled glove box—equipped with an external molecular sieves purification system—and added to the potentiometric cell. The water content of the glove box measured with a Panametric standard hygrometer P1 was ca. 5 ppm. In a few cases the composition of the melt was changed by electrolysis. The apparatus consisted of a controlled-current, controlled-time device (chronoamperostat). The current was controlled with an operational amplifier/transistor circuit to an accuracy of 0.2% and the time period with a preset electromechanical counter by the mains frequency (50 Hz).

Results and Discussion

Determination of the Solubility of KCl in $KFeCl_4$. It has been shown[6] that close to the 1:1 composition in the KCl–$AlCl_3$

Table I. Values of Mole Fraction and Cell Potential for Molten KCl–$FeCl_3$ in the Temperature Range 275–350°

Mole fraction of KCl	$-\Delta E$, mV			
	275°	300°	325°	350°
0.4744_9	488.8	487.7	487.5	488.0
0.4777_8		481.0		
0.4827_1	468.8	467.3	465.7	464.4
0.4869_4	455.4_5	452.9	450.6	448.8
0.4903_6	439.6	437.3	433.8	431.6
0.4935_5	421.2	417.6	413.4	409.9
0.5067_3		55.38		
0.5121_4		26.87		
$0.5125_9{}^a$	14.17	24.31	33.63	43.62
$0.5146_0{}^a$	7.94	17.60	26.78	36.37
0.5160_7	2.95	11.90		30.86
0.5173_7		9.37		
0.5196_3		2.66	11.50	18.31
0.5226_6			4.00	11.19

[a] Produced by electrolysis.

Table II. Composition of $KFeCl_4$ Melts Saturated with KCl in the Temperature Range 275–350°

Temp, °C	Calcd mole fraction of total KCl	pCl^-	Variance × 10^7
275.0 ± 0.3	0.5180 ± 0.0002	0.263 ± 0.002	0.144
300.0 ± 0.3	0.5207 ± 0.0001	0.184 ± 0.002	0.254
325.0 ± 0.3	0.5243 ± 0.0001	0.117 ± 0.002	0.218
350.0 ± 0.3	0.5271 ± 0.0001	0.059 ± 0.003	0.663

system (from 47 to about 52 mol % KCl) the potential of the used concentration cell is (within the experimental uncertainty) given by

$$\Delta E = -\frac{RT}{F} \ln \frac{[\mathrm{Cl}^-]_{\mathrm{II}}}{[\mathrm{Cl}^-]_{\mathrm{I}}} \tag{1}$$

where $[Cl^-]_I$ and $[Cl^-]_{II}$ are the chloride activities in cell compartments I and II, respectively. This can be rewritten as

$$\mathrm{pCl_I^-} = -(F/(RT \ln 10))\Delta E + \mathrm{pCl^-_{II}} \tag{2}$$

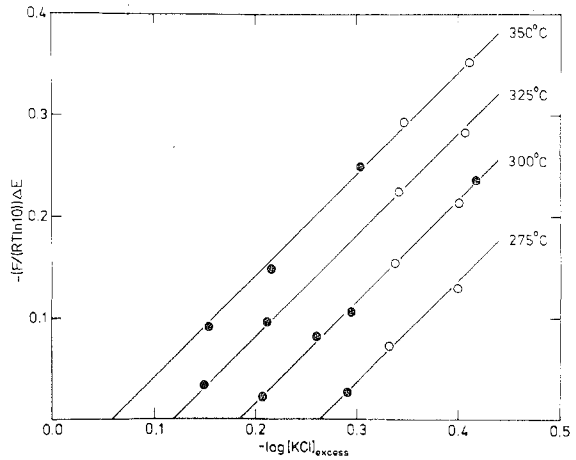

Figure 1. Plots used to obtain the pCl^- for KCl–$FeCl_3$ melts saturated with KCl at 275, 300, 325, and 350°: filled circles, change in melt composition made by weighings; open circles, change made by electrolysis.

where pCl^-_{II} is the pCl^- in the saturated melt; in the present work pCl^- is defined as the negative logarithm of the chloride concentration, since under the present circumstances the chloride activity is assumed equal to the chloride concentration. In order to determine the pCl^- of the saturated melt it was necessary to determine the solubility of KCl in the melt. At high chloride concentration and on the basis of the discussion in the Introduction it should be safe to assume that $FeCl_4^-$ is the only iron complex in the melt. Therefore, an addition of KCl gives rise to an equivalent amount of chloride ions. Thus if $-(F/(RT \ln 10))\Delta E$ for the measurements obtained at mole fractions of KCl higher than 0.500 (values collected in Table I) is plotted against the negative logarithm of the excess formality of KCl, one should (at any given temperature in the working range) obtain a straight line with a slope of unity. The intercept at the abscissa (where $-\Delta E = 0$) should give pCl^-_{II} at the chosen temperature. Such plots are shown in Figure 1. Here the straight lines are drawn on the basis of a least-squares method with the slope fixed at unity. However, if the slope is allowed to vary, one obtains values close to unity. As an average of the slopes at the temperatures 275, 300, 325, and 350° the value 1.01 ± 0.01 (standard error) is obtained. From Figure 1 the composition of the saturated melt at the measured temperatures can be calculated. The results are shown in Table II. The variances given in this table are calculated from the deviations in mole fractions between the measured points and the calculated straight lines. The obtained results are in reasonable agreement with the phase diagram given by Cook and Dunn.[8] A linear extrapolation down to the eutectic temperature of 242°[8] using the weighted data gives a composition of the eutectic mixture of 51.23 ± 0.03 mol % KCl. An extrapolation using the equation $x = e^{A-B/T}$ for the same weighted data, where x is the mole fraction of KCl in the system KCl–$KFeCl_4$ and A and B are parameters obtained by minimizing the deviation (least-squares) between the measured and calculated values, gave as a result a composition for the eutectic mixture of 51.32 ± 0.02 mol % KCl. By comparison the value given by Cook and Dunn was 52 mol % KCl.

Measurements and Calculations for Cell Potentials in the $FeCl_3$–KCl System. If the electrodes discussed above are used for a large compositional range and the pCl^-—calculated from the cell measurements—is plotted against the mole fraction of KCl, an S curve is obtained similar in shape to the S curve found for the KCl–$AlCl_3$ system.[6] The shape of this curve has been shown to be due primarily to the acid–base reaction $2AlCl_4^- \rightarrow Al_2Cl_7^- + Cl^-$. In order to examine what kind of equilibrium was present in the melt, the data given in Table I for the mole fraction of KCl smaller than 0.500 were fitted to model reactions of the form

$$n\mathrm{FeCl_4^-} \rightleftarrows \mathrm{Fe}_n\mathrm{Cl}_{3n+m}{}^{m-} + (n-m)\mathrm{Cl}^- \tag{3}$$

where n and m are integers. n was allowed to vary in the range $1 \leq n \leq 5$ and m was allowed to vary in the range $0 \leq m < n$. This corresponds to a maximum degree of polymerization of 5 and a charge from zero to 4–. A survey of all these models is shown in Table III and in order of increasing polymerization. The best pK as well as the variance based on the deviations in mole fraction is given for each model at each of the measured temperatures. From this table it is clear that the first shown equilibrium (i.e., $FeCl_4^- \rightleftarrows FeCl_3 + Cl^-$) gives the best fit at all temperatures examined. The variances for this equilibrium are of the same size as the variances calculated for the systems with mole fraction of KCl higher than 0.500, where only K^+, $FeCl_4^-$, and Cl^- are present (Table II). An F test ($F = v_1/v_2$, where v_2 is the experimental variance from Table II) shows that the variance ratios for the best fit equilibrium (i.e., $FeCl_4^- \rightleftarrows FeCl_3 + Cl^-$) at all temperatures are above the 30% probability points, whereas the variance ratios for the next best fit equilibrium (i.e., $2FeCl_4^- \rightleftarrows Fe_2Cl_7^- + Cl^-$) at all temperatures are below the 2.5% probability points. A graphical comparison between some of the models at 300° is shown in Figure 2.

It is well known that in the given temperature range ferric chloride is present as the dimeric molecule Fe_2Cl_6 in the vapor phase. In order to dissociate Fe_2Cl_6 in the melt some kind

Table III. Comparison between Different Models for the System KCl-$FeCl_3$ at Different Temperatures

Complex in equilibrium with $FeCl_4^-$ and Cl^-	275°		300°		325°		350°	
	p*K*	Variance × 10^7	p*K*	Variance × 10^7	p*K*	Variance × 10^7	p*K*	Variance × 10^7
$FeCl_3$	5.722	0.341	5.441	0.179	5.189	0.409	4.967	0.999
Fe_2Cl_6	11.6	258	11.0	200	10.5	262	10.1	278
$Fe_2Cl_7^-$	6.53	8.75	6.24	8.33	5.98	8.14	5.76	6.74
Fe_3Cl_9	17.4	608	16.5	474	15.7	614	15.1	641
$Fe_3Cl_{10}^-$	12.4	160	11.8	128	11.3	164	10.8	175
$Fe_3Cl_{11}^{2-}$	7.3	53.1	7.0	49.9	6.7	521	6.5	495
Fe_4Cl_{12}	23.1	877	21.9	694	20.9	882	20.1	913
$Fe_4Cl_{13}^-$	18.1	485	17.3	380	16.5	491	15.8	515
$Fe_4Cl_{14}^{2-}$	13.1	71.1	12.5	59.2	12.0	73.2	11.5	78.7
$Fe_4Cl_{15}^{3-}$	8.0	126	7.6	122	7.4	125	7.2	122
Fe_5Cl_{15}	28.8	1067	27.3	862	26.1	1071	25.0	1100
$Fe_5Cl_{16}^-$	23.9	767	22.7	600	21.7	773	20.8	804
$Fe_5Cl_{17}^{2-}$	18.9	346	18.0	278	17.2	352	16.5	370
$Fe_5Cl_{18}^{3-}$	13.8	18.1	13.3	15.4	12.7	18.8	12.3	20.2
$Fe_5Cl_{19}^{4-}$	8.6	206	8.2	203	8.0	205	7.7	205

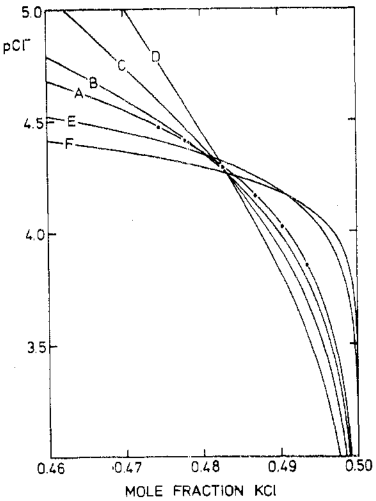

Figure 2. Measured pCl^- values (filled circles) as a function of mole fraction of KCl in KCl-$FeCl_3$ melts at 300° compared with calculated values (full lines) for a series of reaction schemes, which were in reasonably good agreement with the experimental data. The third species in equilibrium with Cl^- and $FeCl_4^-$: A, $FeCl_3$; B, $Fe_2Cl_7^-$; C, $Fe_3Cl_{11}^{2-}$; D, $Fe_4Cl_{15}^{3-}$; E, Fe_2Cl_6; F, Fe_3Cl_9.

Table IV. p*K* Values for the Equilibria $2FeCl_4^- \rightleftarrows Fe_2Cl_7^- + Cl^-$ (1) and $Fe_2Cl_7^- \rightleftarrows Fe_2Cl_6 + Cl^-$ (2) in Molten $KFeCl_4$ Based on Cell Potentials

Temp, °C	pK_1	pK_2	Variance × 10^7
275.0 ± 0.3	6.603 ± 0.005	5.70 ± 0.04	0.121
300.0 ± 0.3	6.322 ± 0.005	5.38 ± 0.03	0.115
325.0 ± 0.3	6.057 ± 0.004	5.18 ± 0.02	0.043
350.0 ± 0.3	5.821 ± 0.006	5.02 ± 0.04	0.126

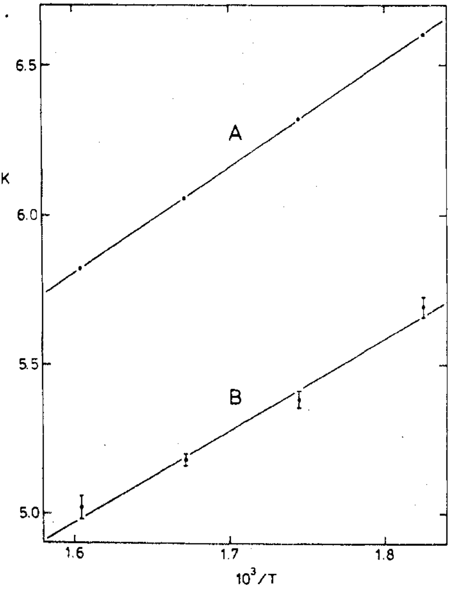

Figure 3. p*K* values as a function of the inverse absolute temperature (×10^3). The straight lines are drawn from a least-squares calculation using weighted values: A, $2FeCl_4^- \rightleftarrows Fe_2Cl_7^- + Cl^-$; B, $Fe_2Cl_7^- \rightleftarrows Fe_2Cl_6 + Cl^-$. The shown limits are based on standard errors.

of complex formation is necessary, for example formation of $Fe_2Cl_7^-$. Therefore the equilibrium $FeCl_4^- \rightleftarrows FeCl_3 + Cl^-$ cannot be of any importance in the melt and calculations involving this equilibrium must just by accident give the best fit. At least two equilibria must be present in the melt. Since an analysis of the spectra for the KCl–$FeCl_3$ system suggests that there are only two iron complexes present in the melt, a third species can only be present in a much lower concentration than the other two species. The main equilibrium therefore must by itself give a reasonably good fit. The only choice seems to be the next best equilibrium in Table III, $2FeCl_4^- \rightleftarrows Fe_2Cl_7^- + Cl^-$, and since there is a fairly high vapor pressure above the melt, the most likely choice for the other equilibrium is $Fe_2Cl_7^- \rightleftarrows Fe_2Cl_6 + Cl^-$. The calculated p*K* values (pK_1 and pK_2) for these two equilibria are given in Table IV. As expected, a very good fit is obtained, but as we have seen before this is not a proof that we are dealing with the actual equilibria. It would be of great value to compare the obtained results with the results from a different method, for example, vapor pressure measurements.

Unfortunately, vapor pressure measurements have not been performed on the KCl–$FeCl_3$ system in the actual measured range. If we, however, look at the NaCl–$FeCl_3$ system,[8] it is possible to get an idea about how good the agreement is between the potentiometric measurements and the vapor pressure measurements. At 300° and at mole fractions of NaCl of 0.484, 0.472, and 0.450 the vapor pressure above the melt is ca. 1.6, 3.5, and 10.6 mm, respectively. The calculated mole fractions of Fe_2Cl_6 (the other components are assumed to be K^+, $FeCl_4^-$, and $Fe_2Cl_7^-$), based on the values given in Table IV, are 0.0019, 0.0063, and 0.0215, respectively. From a plot of vapor pressure vs. composition it can be seen that Henry's law seems to be followed. The calculated vapor pressures based on Raoult's law (the vapor pressure of molten ferric chloride at 300° is assumed to be ca. 570 mm[9]) are 1.1, 3.6, and 12.3 mm, respectively.

As expected the p*K* value for the reaction $2FeCl_4^- \rightleftarrows Fe_2Cl_7^- + Cl^-$ at 300° is smaller than the p*K* value for the reaction $2AlCl_4^- \rightleftarrows Al_2Cl_7^- + Cl^-$,[6] showing that $AlCl_4^-$ is

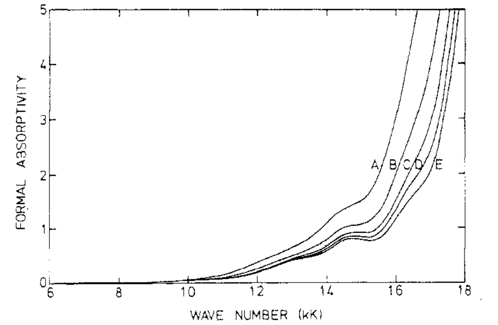

Figure 4. Series of spectra of the KCl-FeCl$_3$ system at 300°. Mole fraction of KCl: A, 0.4570_0; B, 0.4804_5; C, 0.4897_7; D, 0.4945_4; E, 0.5074_6. The formal absorptivity is based on the concentration of Fe(III).

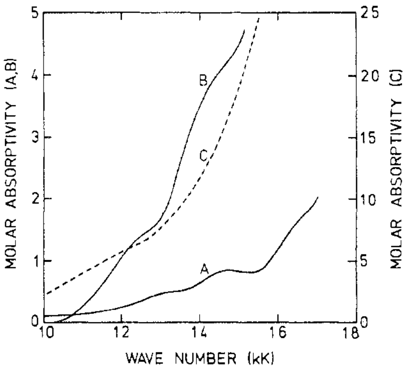

Figure 5. Calculated spectra for the KCl-FeCl$_3$ system at 300°: A, FeCl$_4^-$; B, Fe$_2$Cl$_7^-$; C, Fe$_2$Cl$_6$. Each spectrum was calculated on the basis of five measured spectra by use of the p*K* values 6.322 and 5.38 for the reactions $2FeCl_4^- \rightleftarrows Fe_2Cl_7^- + Cl^-$ and $Fe_2Cl_7^- \rightleftarrows Fe_2Cl_6 + Cl^-$, respectively.

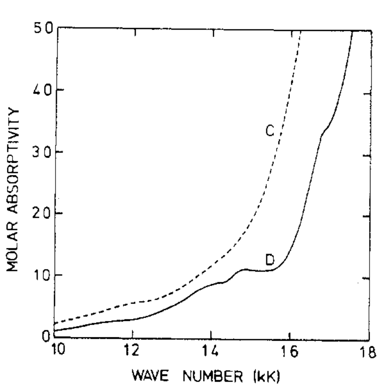

Figure 6. Comparison of (C) the "calculated" spectrum of Fe$_2$Cl$_6$ in KFeCl$_4$ and (D) the measured spectrum of Fe$_2$Cl$_6$ in the gaseous phase at 300°.

more stable than FeCl$_4^-$ (i.e., at the same pCl$^-$ and temperature a higher percentage of the total Al(III) is in the AlCl$_4^-$ form than the percentage of Fe(III) in the FeCl$_4^-$ form). Furthermore, the p*K* should vary in an inversely proportional manner with the absolute temperature. That this is the case can be seen in Figure 3. From this figure the $\Delta H°$ for the reaction $2FeCl_4^- \rightarrow Fe_2Cl_7^- + Cl^-$ in KFeCl$_4$ was found by a weighted least-squares method to be 16.33 ± 0.07 kcal/mol, and the $\Delta S°$ was found to be 0.4 ± 0.1 cal/(deg mol). Similarily $\Delta H°$ was found to be 14 ± 1 kcal/mol and $\Delta S°$ was found to be 0 ± 2 cal/(deg mol) for the reaction $Fe_2Cl_7^- \rightarrow Fe_2Cl_6 + Cl^-$ also in the temperature range 275–350°. According to the calorimetric work by Cook and Dunn[8] the extrapolated value of $\Delta H°$ for the reaction $KFeCl_4(l) \rightarrow FeCl_3(l) + KCl(l)$, where no solvent is present, should be about 16.5 kcal/mol in the same temperature range. For comparison $\Delta H°$ for the reaction $FeCl_4^- \rightarrow {}^1/_2Fe_2Cl_6 + Cl^-$ can be calculated from the values given above to be 15.2 ± 0.5 kcal/mol.

Spectra. In Figure 4 are shown some spectra for the KCl–FeCl$_3$ system at 300°. An analysis of these spectra suggests that they are internally linearly dependent and therefore there can be only two iron complexes present in the melt. However, small amounts of another species cannot be excluded.

It can be shown[13] that if we deal with *m* different spectra obtained at *m* different compositions, a general equation involving three matrices can be put forward, i.e.

$$[c_{mi}][\epsilon_i(\nu_n')] = A_m(\nu_n')/l \tag{4}$$

where c_{mi} is the concentration of the *i*th species for the *m*th composition, $\epsilon_i(\nu_n')$ is the absorptivity of the *i*th species at the wave number ν_n', $A_m(\nu_n')$ is the total absorbance of the *m*th composition at the wave number ν_n', and *l* is the path length. In the present case ν_n' was measured at 238 different wave numbers in the range 10.0–17.0 kK. If the values of pK_1 and pK_2 at 300° are used in eq 4, the spectra of FeCl$_4^-$, Fe$_2$Cl$_7^-$, and Fe$_2$Cl$_6$ can be calculated from the five spectra shown in Figure 4. The results is shown in Figure 5. A comparison of the calculated spectrum of pure FeCl$_4^-$ in KCl–FeCl$_3$ with the spectrum of (C$_2$H$_5$)$_4$NFeCl$_4$ in acetone, where bands are found at 13.70, 14.60, 16.15, and 16.70 kK,[18] shows that the same complex is probably present in the two systems. The molar absorptivity for (C$_2$H$_5$)$_4$NFeCl$_4$ in acetone varies from 0.2 to 0.6 in the range 12–17 kK, whereas the molar absorptivity for FeCl$_4^-$ in KCl–FeCl$_3$ varies from 0.2 to 1.8. However, at the higher temperature a foot of a charge-transfer band probably reaches into the measured wave number range.

The error in the calculated spectrum of Fe$_2$Cl$_6$ is of course rather large since the concentration of Fe$_2$Cl$_6$ is very low. A comparison of the calculated spectrum of Fe$_2$Cl$_6$ at 300° and Fe$_2$Cl$_6$ in the vapor phase at 300° is given in Figure 6. In order to secure that Fe$_2$Cl$_6$ was present in the vapor phase $^1/_{10}$ atm of Cl$_2$ was (at room temperature) added to the optical cell. The vapor pressure of Fe$_2$Cl$_6$ in the cell (a solid phase was present) was obtained from the work by Johnstone et al.[9] As can be seen in Figure 6 there is some resemblance between the calculated spectra of Fe$_2$Cl$_6$ in the melt and Fe$_2$Cl$_6$ in the gaseous phase, but it is not possible to prove or disprove anything on this basis, especially in view of the error in the calculated spectra.

Acknowledgment. The authors wish to thank B. Lottrup-Knudsen for help with programming and C. E. Foverskov for designing the electronic apparatus to our requirements. Further thanks are due to Carlsbergfondet for financial support and to the Northern Europe University Computing Center (NEUCC) for computing time.

Registry No. FeCl$_3$, 7705-08-0; KCl, 7447-40-7; KFeCl$_4$, 15274-97-2; Fe$_2$Cl$_7^-$, 12442-73-8; Fe$_2$Cl$_6$, 16480-60-7.

References and Notes

(1) B. Trémillon and G. Letisse, *J. Electroanal. Chem. Interfacial Electrochem.*, **17**, 371, 387 (1968).
(2) G. Torsi and G. Mamantov, *Inorg. Chem.*, **10**, 1900 (1971).
(3) A. A. Fannin, Jr., L. A. King, and D. W. Seegmiller, *J. Electrochem. Soc.*, **119**, 801 (1972).
(4) G. Torsi and G. Mamantov, *Inorg. Chem.*, **11**, 1439 (1972).
(5) L. G. Boxall, H. L. Jones, and R. A. Osteryoung, *J. Electrochem. Soc.*, **120**, 223 (1973).
(6) J. H. von Barner and N. J. Bjerrum, *Inorg. Chem.*, **12**, 1891 (1973).
(7) T. Sato, T. Ishikawa, and R. Midorikawa, *Denki Kagaku*, **41**, 123 (1973).
(8) C. M. Cook, Jr., and W. E. Dunn, Jr., *J. Phys. Chem.*, **65**, 1505 (1961).
(9) H. F. Johnstone, H. C. Weingartner, and W. E. Winsche, *J. Am. Chem. Soc.*, **64**, 241 (1942).
(10) I. S. Morozov and D. Ya. Toptygin, *Zh. Neorg. Khim.*, **2**, 2129 (1957).
(11) M. D. Pyatunin, A. V. Storonkin, and I. V. Vasilkova, *Vestn. Leningr. Univ., Fiz., Khim.*, **73**, 165 (1973).
(12) R. R. Richards and N. W. Gregory, *J. Phys. Chem.*, **69**, 239 (1965).
(13) K. Tempelhoff, H.-H. Emons, and W. Meisel, *Z. Anorg. Allg. Chem.*, **372**, 1 (1970).

(14) R. S. Juvet, Jr., V. R. Shaw, and M. A. Khan, *J. Am. Chem. Soc.*, **91**, 3788 (1969).
(15) J. H. von Barner, N. J. Bjerrum, and K. Kiens, *Inorg. Chem.*, **13**, 1708 (1974).
(16) S. N. Flengas and A. Block-Bolten, "Advances in Molten Salt Chemistry", Vol. 2, J. Braunstein, G. Mamantov, and G. P. Smith, Ed., Plenum Press, New York, N.Y., 1973, pp 43, 44.
(17) H. A. Andreasen, N. J. Bjerrum, and C. E. Foverskov, to be submitted for publication.
(18) S. Balt, *Recl. Trav. Chim. Pays-Bas*, **86**, 1025 (1967).

Contribution from the Department of Chemistry,
University of Michigan, Ann Arbor, Michigan 48104

Electronic Spectrum of the Tetrachloronickelate(II) Complex at 2.2°K

VAUGHN J. KOESTER[1] and T. M. DUNN*

Received January 7, 1975 AIC500195

The single-crystal electronic spectrum of bis(tetraethylammonium) tetrachloronickelate(II), $(Et_4N)_2NiCl_4$, containing tetragonally distorted $NiCl_4^{2-}$ tetrahedra, was obtained at 2.2°K. Transitions to all the possible crystal field terms arising from the configuration d^8 were identified with the exception of the transition terminating on the ^1A level arising from the free-ion ^1S term. In the strongly absorbing red region, the polarized single-crystal spectrum of Cs_3ZnCl_5 doped with Ni^{2+} was also obtained. Electronic transitions are assigned on the basis of a semiempirical calculation performed within the framework of the crystal field model for tetrahedral coordination. Effects on the spectrum due to spin–orbit coupling and tetragonal distortion are analyzed and discussed. The large splitting in the $^3T_1(^3P)$ manifold is assigned as being due to these combined effects. The emission spectrum of $(Et_4N)_2ZnCl_4$ doped with Ni^{2+} was obtained at 2.2°K. A progression in an Et_4N^+ fundamental, based on $NiCl_4^{2-}$ electronic and vibronic origins, is taken as evidence for significant anion to cation coupling in the crystal.

Introduction

The electronic absorption spectra of tetrahedral complexes of Ni^{2+} have been studied extensively.[2-15] The most detailed analyses were performed on spectra of single-crystal (host) materials doped with nickel and cooled to approximately 4°K.[8,10,12,15] In the earlier investigations, using oxide and sulfide hosts,[8,10,12] the presence of complicated phonon structure prevented a detailed analysis of the spectra. Host materials which contain discrete tetrahedral moieties can be used to minimize this difficulty and recently the polarized absorption spectrum of the $NiCl_4^{2-}$ species in a Cs_3MgCl_5 host was obtained.[15]

The strongest band system in the red region has been assigned in all cases to the $^3T_1(^3P) \leftarrow {}^3T_1(^3F)$ transition on the basis of semiempirical crystal field calculations. Effects due to spin–orbit coupling and lower symmetry fields were also considered, particularly by Couch and Smith.[15]

Since, in previous investigations, spectra were obtained with relatively dilute crystals, only the strongest transitions have been characterized. For this reason, we have obtained the absorption spectrum of the $NiCl_4^{2-}$ complex using the pure $(Et_4N)_2NiCl_4$ compound which allows observation of several very weak electronic transitions.

The crystal field energy level pattern for tetrahedral Ni^{2+} (d^8) was calculated by Liehr and Ballhausen[16] (abbreviated LB). Their calculation parameterized the spin–orbit coupling in terms of the term constant λ and expressed the electron repulsion in terms of the Slater–Condon–Shortley F_2 and F_4 parameters. The parameter values used by LB were $\lambda = -275$ cm^{-1}, $F_2 = 14F_4$, and $F_4 = 90$ cm^{-1} and a similar diagram is shown in Figure 1. This diagram shows the ground state, derived from the $^3T_1(^3F)$ state, to be Γ_1, and separated from the next lowest level by a large enough energy so that, at 4°K, only Γ_1 is occupied. In T_d symmetry the transition $\Gamma_5 \leftarrow \Gamma_1$ is allowed (T_d notation). In the compounds being investigated the site symmetry of the $NiCl_4^{2-}$ complex is D_{2d}, so that $\Gamma_1 \rightarrow A_1$ and $\Gamma_5 \rightarrow E + B_2$; i.e., we have the electric dipole selection rules $E \leftarrow A_1$ and $B_2 \leftarrow A_1$. Calculations of the LB type were used in making a preliminary assignment of the spectrum.

In T_d symmetry there are four fundamental vibrations of the $NiCl_4^{2-}$ moiety. These are designated as $\nu_1(a_1)$, $\nu_2(e)$, $\nu_3(t_2)$, and $\nu_4(t_2)$. Infrared spectra give the $\nu_3(t_2)$ and $\nu_4(t_2)$ fundamentals at 289 and 112 cm^{-1}, respectively.[17,18] From the $ZnCl_4^{2-}$ Raman spectrum[19] in the compound $(Et_4N)_2ZnCl_4$, the $\nu_1(a_1)$ and $\nu_2(e)$ frequencies are determined to be 280 and 60 cm^{-1}, respectively. It is expected that the $NiCl_4^{2-}$ $\nu_1(a_1)$ and $\nu_2(e)$ fundamentals are approximately equal to these values. Indeed the $\nu_2(e)$ fundamental was tentatively assigned at 79 cm^{-1}.[18] In D_{2d} we designate a vibration according to the T_d fundamental from which it is derived; e.g., $\nu_2(e)$ gives rise to $a_1(\nu_2)$ and $b_1(\nu_2)$.

Experimental Section

1. $(Et_4N)_2NiCl_4$ and $(Et_4N)_2ZnCl_4$. Since the preparations of the zinc and nickel compounds are identical, only the nickel compound will be discussed. These compounds were previously characterized by Gill and Nyholm[4] and their methods were followed precisely.

A solution of the complex in absolute EtOH was slowly evaporated in a desiccator containing concentrated H_2SO_4, and single crystals suitable for spectroscopic analysis were obtained. The crystals were stored in a desiccator or under Nujol because of their deliquescent nature.

The crystal system to which $(Et_4N)_2NiCl_4$ belongs is tetragonal.[20] Its space group is $P4_2/nmc$ (D_{4h}^{15}) with two formula units per unit cell. This compound has been shown to be isomorphous with the $(Et_4N)_2ZnCl_4$ salt.[17,21] In both cases the MCl_4^{2-} species exist as discrete molecular units with a site symmetry at each nickel position of D_{2d}. The molecule is situated such that the *c* crystallographic axis bisects the smaller Cl–Ni–Cl angle and coincides with the *z* cartesian axis of the D_{2d} point group. In addition, the *x* and *y* cartesian axes of the D_{2d} point group are rotated by 45° with respect to the *a* and *b* crystallographic axes.

The structure also appears to be disordered in such a way that the exact nuclear geometry of the $NiCl_4^{2-}$ species is uncertain. Any distortion from D_{2d} symmetry, however, is apparently very small and, on the average, D_{2d} symmetry is maintained at the nickel sites.

2. $(Et_4N)_2Zn(Ni)Cl_4$. Sufficient quantities of $(Et_4N)_2NiCl_4$ and $(Et_4N)_2ZnCl_4$ were added to absolute alcohol to saturate the solution at its boiling point. The solution was filtered and the EtOH was added to the filtrate to dissolve the precipitate which formed. Slow evaporation yielded very small light blue single crystals. The nickel concentration was not precisely determined. Since the crystal size